International Forum on Aeroelasticity and Structural Dynamics
IFASD 2022
13-17 June 2022, Madrid, Spain

AEROELASTIC TAILORING OPTIMISATION OF A COMBAT AIRCRAFT WING WITH TOW-STEERED COMPOSITES

A. Tatar[1], R. C. M. Cheung[1], J.E. Cooper[1], D.P. Pearson[2], and C. Warsop[3]

[1] Department of Aerospace Engineering,
University of Bristol, Bristol, BS8 1TR, United Kingdom
ali.tatar@bristol.ac.uk, r.c.m.cheung@bristol.ac.uk, j.e.cooper@bristol.ac.uk

[2] BAE Systems
Warton Aerodrome, Warton, Preston, PR4 1AX, United Kingdom
david.p.pearson@baesystems.com

[3] BAE Systems
Filton, Bristol, BS34 7QW, United Kingdom
clyde.warsop@baesystems.com

Keywords: aeroelastic tailoring, tow-steering, aeroelastic optimization, combat aircraft wing

Abstract: This paper investigates the possibility of employing tailored unidirectional and fibre steered aeroelastically tailored composite lay-up techniques for a combat aircraft wing to meet performance requirements (maximise lift/drag) at more than one design condition whilst still satisfying aeroelastic and structural constraints, with particular emphasis on desired camber / twist schedules. A finite element model of the combat aircraft wing is presented and then, static aeroelastic analysis and modal analysis are carried out to understand the underlying structural and aeroelastic behaviour. Following the definition of a baseline "black metal" (BM) results, a design case exploration for unidirectional (UD) rotated composite layers is performed. After these initial studies, an in-house passive aeroelastic tailoring optimisation code has been developed in MATLAB 2020a incorporating Nastran 2018 gradient-based algorithms to minimise the wing weight, subject to a range of aeroelastic and structural constraints, through the optimisation of thickness distribution and ply angle orientation. Unidirectional, 1D Variable Angle Tow (VAT) and 2D Variable Angle Tow design strategies are considered, and the results compared to the baseline BM case. It is found that weight reduction could be achieved using the UD, 1D VAT and 2D VAT design approaches with up to 35% achieved in the latter case compared to the baseline. This study demonstrates the potential of using passive aeroelastic tailoring for wing structural design and suggests a pathway toward practical passive aeroelastic wing designs.

1 INTRODUCTION

Aeroelastic tailoring in aircraft wing and wind turbine blade design processes involves the exploitation of anisotropic composite characteristics to passively optimise the aeroelastic performance across all possible missions [1,2]. In composite aircraft wings, this aim is commonly achieved by changing the directional properties of the composite material, as initially described in the early 1980s using unidirectional changes in each laminate layer [3,4]. In aerospace and wind engineering, it has been shown how the use of tow steered composites,

designing the laminar orientations as a function of position on the wing, can provide better aeromechanical and dynamic performance [5–10].

Since the beginning of millennium, the widely known technology called " tow-steering" has been developed in order to produce composite laminates with variable angle tow (VAT) plies [11]. In principle, composite tow steering allows tailoring of the stiffness and bend-twist coupling along the wing. For a basic beam, the coupled bending-torsional equation can be written as

$$\begin{bmatrix} M_b \\ T_b \end{bmatrix} = \begin{bmatrix} EI & -K_c \\ -K_c & GJ \end{bmatrix} \begin{bmatrix} w'' \\ \theta' \end{bmatrix} \tag{1}$$

where EI, GJ and K_c represent the bending, torsional and bending-torsional coupling rigidities, and M_b and T_b represent the bending and twisting moments, respectively. This equation demonstrates the main philosophy behind passive aeroelastic tailoring of wings where variation in the composite ply angle orientation along the wing introduces variable bending-torsional coupling through the K_c parameter, enabling structural and aeroelastic performance of wing structures to be improved. For example, the coupling rigidity term can directly affect wash-out (leading to reduction in angle of attack in the wing section) and wash-in (leading to increase of angle of attack in the wing section) parameters in the wing. Variation of K_c is achieved through exploitation of the anisotropic composite properties via the lay-up orientations.

In aircraft wing structures, tow-steering can be divided into three main groups: (i) local tow-steering, (ii) regional tow steering and (iii) global tow steering. For instance, local tow-steering can be used to improve buckling resistance and reduce stress concentrations in specific areas with minimum mass increase, whereas regional tow-steering can be employed to improve control effectiveness by changing the stiffness distribution around a control surface. The most used approach, global tow-steering, is employed for maximising overall effects such the lift-to-drag ratio, improving flutter and divergence speed, and facilitating manoeuvre and gust loads alleviation [12].

Most optimisation studies on passive aeroelastic tailoring wings are carried out to increase flutter and divergence speeds, decrease wing weight and increase lift generation by considering the aeroelastic constraints [5,6]. The aeroelastic tailoring problem is a multi-disciplinary optimisation challenge. Although there have been a number of studies carried out on passive aeroelastic tailoring wings for different type of civil aircraft and experimental structures [12–14], more research is required for understanding the benefits of passive aeroelastic tailoring on combat aircraft wings. This paper describes how to develop passive aeroelastic design methodologies, including tailored unidirectional and fibre steered designs, and to gain an initial appreciation of their application to a representative aeroelastic combat aircraft wing structure.

2 WING MODEL DESCRIPTION

2.1 Structural Model

The finite element (FE) model of the representative aircraft wing is created by BAE Systems in-house software "FEWinGen" to understand its structural and aeroelastic behaviour, as shown in Figure 1.

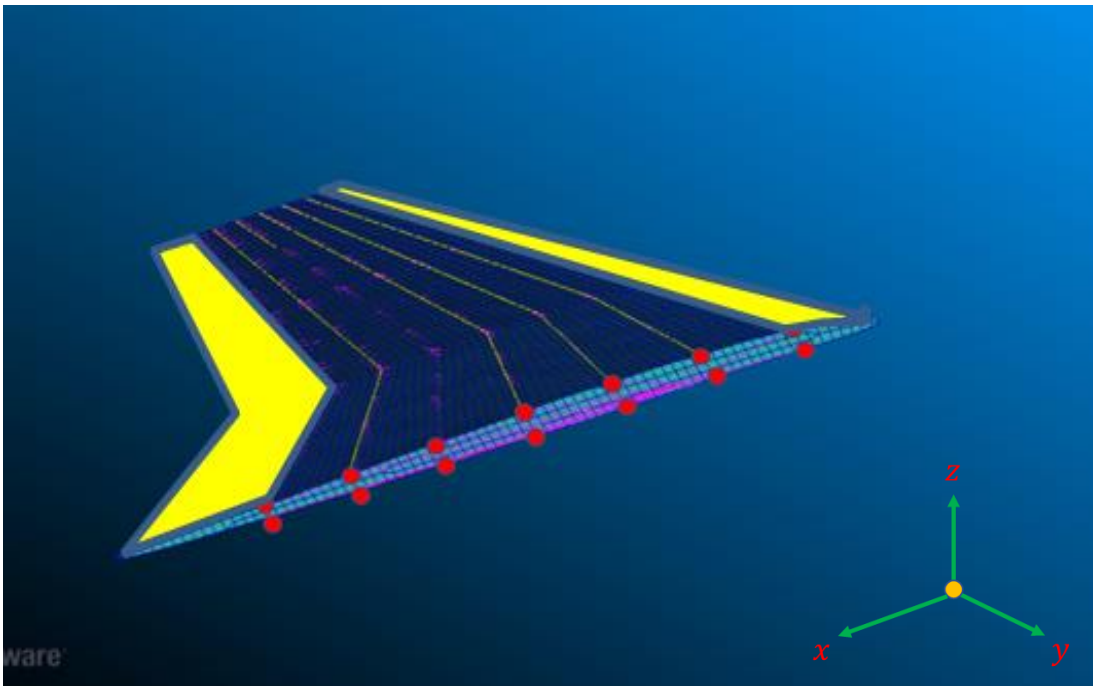

Figure 1: Structural FE model of the combat aircraft wing.

The structural FE model mainly consists of ribs, spars, upper and lower skins. All spars and ribs are modelled with CQUAD4 and CTRIA3 shell elements, consisting of isotropic metallic elements. The lower and upper skins are modelled with CQUAD4 and CTRIA3 shell and composite laminate elements. It should be noted that composite laminates on the lower and upper skins are defined between front (leading edge side) and rear (trailing edge side) spar, and the leading and trailing edge elements are metallic. The leading edge (LE) and trailing edge (TE) regions in the FE model are filled with 3D CHEXA and CPENTA solid elements with having properties of foam in order to stabilise the optimised structure. CBAR elements are also used for spar modelling in addition to CQUAD4 and CTRIA3 shell elements. The displacement of all spars is constrained at the root of the wing for idealising the wing root attachment. A summary of the elements making up the FE model is presented in Table 1.

Table 1: FE model summary.

Entry Name	Number of Entries	Entry Name	Number of Entries
CBAR	728	MAT8	1
CQUAD4	5680	PBAR	728
CTRIA3	133	PCOMP	3182
GRID	5243	PSHELL	2631
MAT1	6	RBE3	28
CHEXA	558	CPENTA	16

The number of composite plies for each element are constant (24) with the ply angle stacking sequence defined as:

(0, 45, 90, -45, 0, 45, 90, -45, 0, 45, 90, -45 / SYM)

This layup, which is black metal, has a quasi-isotropic behaviour when considered along the wing surface. Carbon fibre composite (CFR) is used as the composite wing skin material. All

plies with the same angle orientation plies have the same thickness, but other orientations may have different thickness. The composite layers, spars and ribs have varying thickness along the wing.

In the leading edge (LE) and trailing edge (TE) regions, PU240 Polyurethane is used as a filling foam material as it is a relatively light stiffening material that has been used in previous aerospace applications [15–18]. Properties of the composite and foam materials used in the optimisation study of combat aircraft wing are given in Table 2.

Table 2: Material properties.

Property	Carbon Fibre Composite	Foam PU240 Polyurethane
Elastic Modulus 11 - E_{11} [GPa]	155	
Elastic Modulus 22 - E_{22} [GPa]	8.4	
Shear Modulus 12 - G_{12} [GPa]	3.2	
Elastic Modulus [GPa]		0.15
Poisson`s Ratio		0.3
Density [kg/m^3]	1628	240

To understand the underlying static and dynamic behaviour of the wing, a series of initial computations were performed. First, considering the dynamic characteristics, a modal analysis was carried out using the Nastran normal mode analysis solver for the idealised the wing root attachment. The first nine vibration modes of the wing are presented in Figure 2. The first three vibration modes are identified as global coupled bending-torsional.

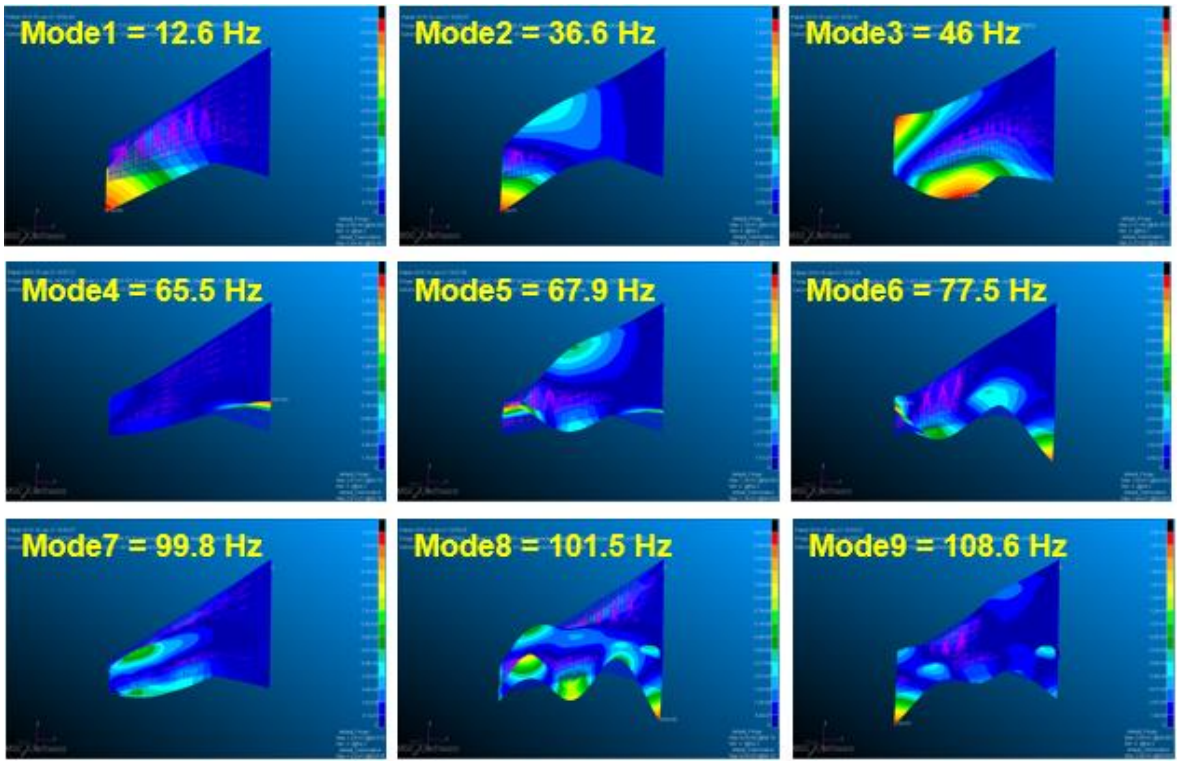

Figure 2: Modal analysis of the combat aircraft wing.

2.2 Aeroelastic Model

For the static aeroelastic analysis of combat aircraft wing, the aerodynamics loads are applied to each node of the FE model. The aerodynamic loads were computed by computational fluid dynamics (CFD) simulations for four different subcases as seen in Table 3. These aerodynamic loads are used in the passive aeroelastic tailoring optimisation studies. Among these four subcases, three of them (subcases 1000, 2000 and 300) are manoeuvre cases whereas subcase 2000 is the cruise case.

Table 3: Aerodynamic load cases.

Subcase #	Configuration	Acceleration [g]	Mach	Altitude [ft]
1000	Manoeuvre Case	6	0.7	0
2000	Cruise Case	1	1.4	36000
3000	Manoeuvre Case	7	0.9	20000
4000	Manoeuvre Case	-3	0.9	20000

A static aeroelastic analyses of the structural FE model was conducted for the aerodynamic load subcase 1000 from Table 3 using static analysis solver in Nastran 2018. In the subcase 1000, the air speed is 0.7 Mach, altitude is sea level and acceleration is 6 g during the manoeuvre. For the original model, the deformation and stress due to the aerodynamic loads are shown in Figures 3a and 3b, respectively. The maximum deformation and major principal stress on the metallic parts were computed as 556 mm and 356 MPa, respectively.

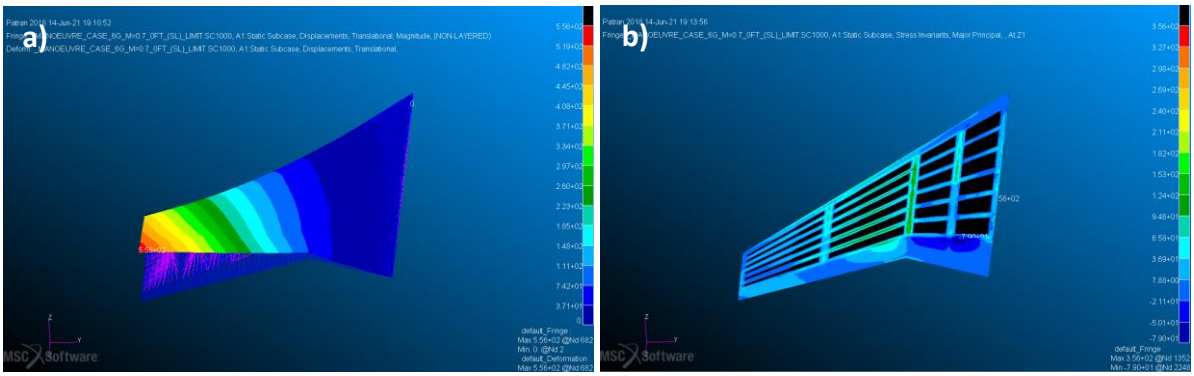

Figure 3: Static aeroelastic response for subcase 1000, a) deformation, b) stress.

3 UNIDIRECTIONAL DESIGN SPACE EXPLORATION

Understanding the unidirectional aeroelastic response of the wing model for different angle orientations is important to get an idea of the deformations and stresses, and also to explore the effect of the initial angle orientation values of optimisation studies, before starting the actual optimisation studies. In this section, design space of the wing model will be explored for the unidirectional angle orientation with the consideration of aeroelastic response.

To implement a robust fibre steering optimisation strategy, including both unidirectional and variable angle tow steering, more “zero” ply angles are required. Therefore, the stacking sequence is modified to (0, 90, 0, 45, 0, -45, 0, 90, 0, 45, 0, -45/ SYM) along the wing surface, making the ply angle proportion as 50% “0°”, 16.7% “90°”, 16.7% “45°”, 16.7% “-45°”. This ply angle proportion is used for the unidirectional design space exploration of the wing model in the following sections. The rotation of this stacking sequence as a uniform block relative to the zero plies not only makes the analysis easier to implement and visualise, but also simplifies

the manufacturing and certification process. The orientations that are referred to in this study relate to the rotation of the entire layup/stack with respect to the initial zero-degree plies.

3.1 Static Aeroelastic Analysis

A case study considering just aerodynamic loads was initially performed to understand the design space for both composite skin thickness and the effect of rotating the composite orientations (all plies rotated by the same amount) on the aeroelastic behaviour. For this purpose, a design of experiments (DoE) matrix was created. Eight different cases for the orientation of the upper and lower skins are used in the DoE matrix, which are presented in Table 4.

Table 4: Case study varying stack orientation.

Case Study	A	B	C	D	E	F	G	H
Upper skin angle orientation [deg]	0	+30	+30	-30	+60	+60	-60	+90
Lower skin angle orientation [deg]	0	+30	-30	+30	+60	-60	+60	+90

Static aeroelastic analyses were conducted for the aerodynamic load subcase 1000 using the static analysis solver (SOL101) in Nastran 2018. Subcase 1000 given in Table 3 was selected as one of the design load cases. For "0" degree unidirectional (UD) orientation Case Study - A, the deformation and stresses due to the aerodynamic loads are plotted in Figure 4. The maximum deformation, tip twist angle and major principal stress in the metallic parts were computed as 606 mm, 7.54 degrees and 412 MPa, respectively. The maximum composite stress for each layer gives an indication of the range of stresses that can occur due to the varying orientations of each composite ply. The maximum major principal stress in the overall structure was found as 926 MPa in the first layer.

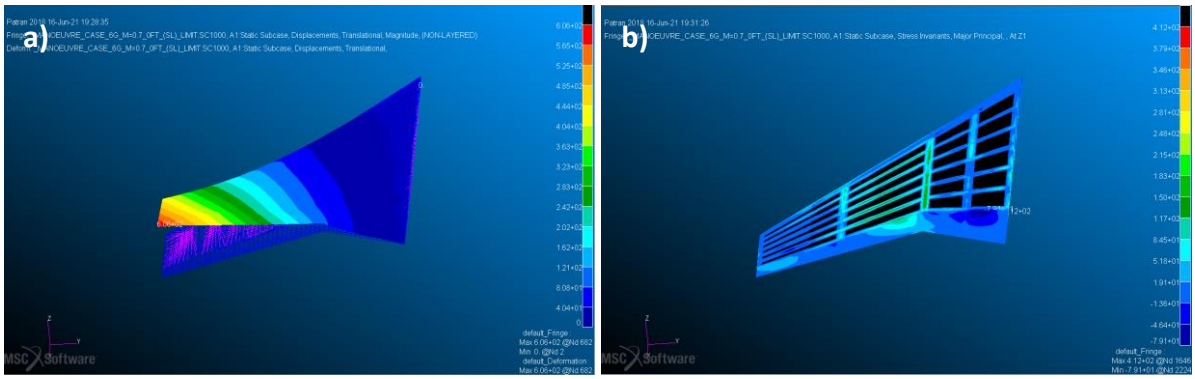

Figure 4: Static aeroelastic response with 0 deg UD angle orientation for subcase 1000, a) deformation, b) stress.

The maximum bending deflection, twist angle at the tip and composite layer stress for different unidirectional angle orientation are shown in Figure 5. Critical cases are found as:

- Maximum deflection = Case C - Upper (+30°) and Lower (-30°)
- Minimum deflection = Case D - Upper (-30°) and Lower (+30°)
- Maximum tip twist = Case A - Upper (0°) and Lower (0°)
- Minimum tip twist = Case G - Upper (-60°) and Lower (+60°)
- Maximum composite stress = Case E - Upper (+60°) and Lower (+60°)
- Minimum composite stress = Case G - Upper (-60°) and Lower (+60°)

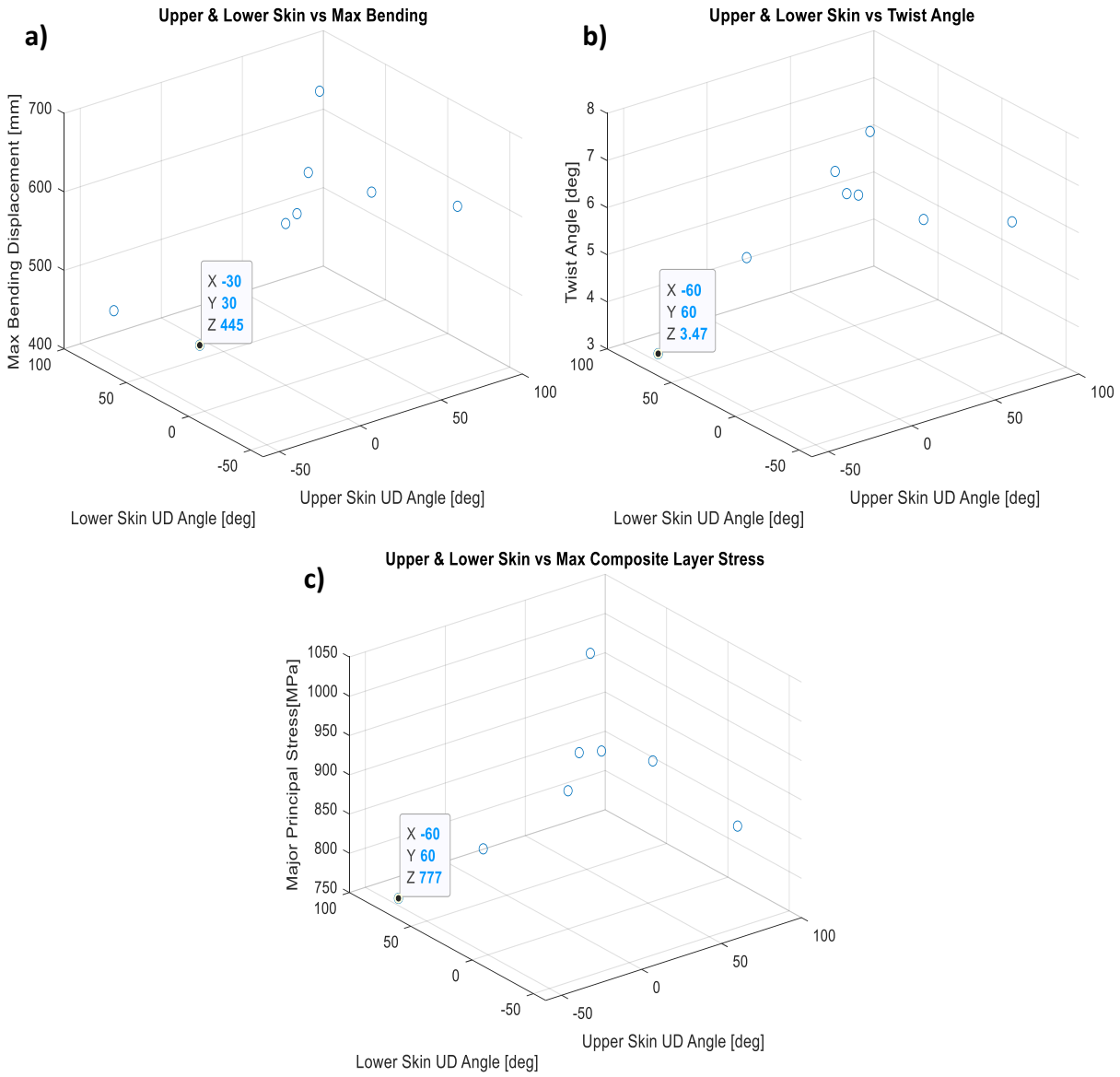

Figure 5: Updated FE model with "0" degree UD angle orientation -subcase 1000, a) maximum bending deflection, b) twist angle at the tip, c) maximum composite layer stress.

3.2 Static Aeroelastic Analysis with Fuel Loads and Ultimate Factor

Static aeroelastic analyses of the updated FE model with "0" degree UD angle orientation was carried out by including fuel loads and then multiplying by the ultimate load factor "1.5". In these analysis, all four subcases were considered.

Table 5: Static aeroelastic response of 1.5 x (CFD + fuel loads) – "0" degree UD orientation.

Subcase #	Maximum deflection [mm]	Tip twist angle [deg]	Major principal stress [MPa]
1000	884	-11	589
2000	262	-3.79	156
3000	662	-8.43	617
4000	469	5.60	301

Table 5 summarises the results in terms of maximum deflection, tip twist angle and major principal stress. It is clearly seen from Table 5 that subcase 1000 results in the highest maximum

deflection and twist angle, and subcase 3000 results in the highest major principal stress in the metallic parts.

Furthermore, three different load configurations which are (i) “Aerodynamic loads only”, (ii) “aerodynamic + fuel loads”, (iii) “1.5 x (aerodynamic+ fuel Loads)” were analysed by conducting static aeroelastic analyses for subcase 1000 in Nastran 2018. The results were then compared in Table 6 in terms of maximum deflection and tip twist angle. As expected, deformation and tip twist angle increase with respect to the ultimate factor. On the other hand, addition of the fuel loads decreases deformation and tip twist angle because of opposite direction of the fuel loads, which is in the direction of gravity. This is the inertial relief provided by the fuel weight.

Table 6: Static aeroelastic response comparison for subcase 1000 – “0” degree UD orientation.

Load Case	Maximum deflection [mm]	Tip twist angle [deg]
Aerodynamic Loads Only	606	-7.54
Aerodynamic + Fuel Loads	589	-7.38
1.5 x (Aerodynamic+ Fuel Loads)	884	-11

3.3 Modal Analysis

For the updated model with “0” degree UD angle orientation, a modal analysis was also conducted to assess the global dynamic behaviour. In a similar manner to the original model with quasi-isotropic composite laminates (black metal) in section 2.1, the first three global bending-torsional modes can be clearly seen in Figure 6. Overall, the mode shapes do not change significantly. However, the frequencies of the first two global modes slightly decrease whereas frequency of the third global mode increases significantly compared to the original model because of the modified ply proportion in “0” degree UD angle orientation. Note that frequency separation generally delays the onset of flutter instability.

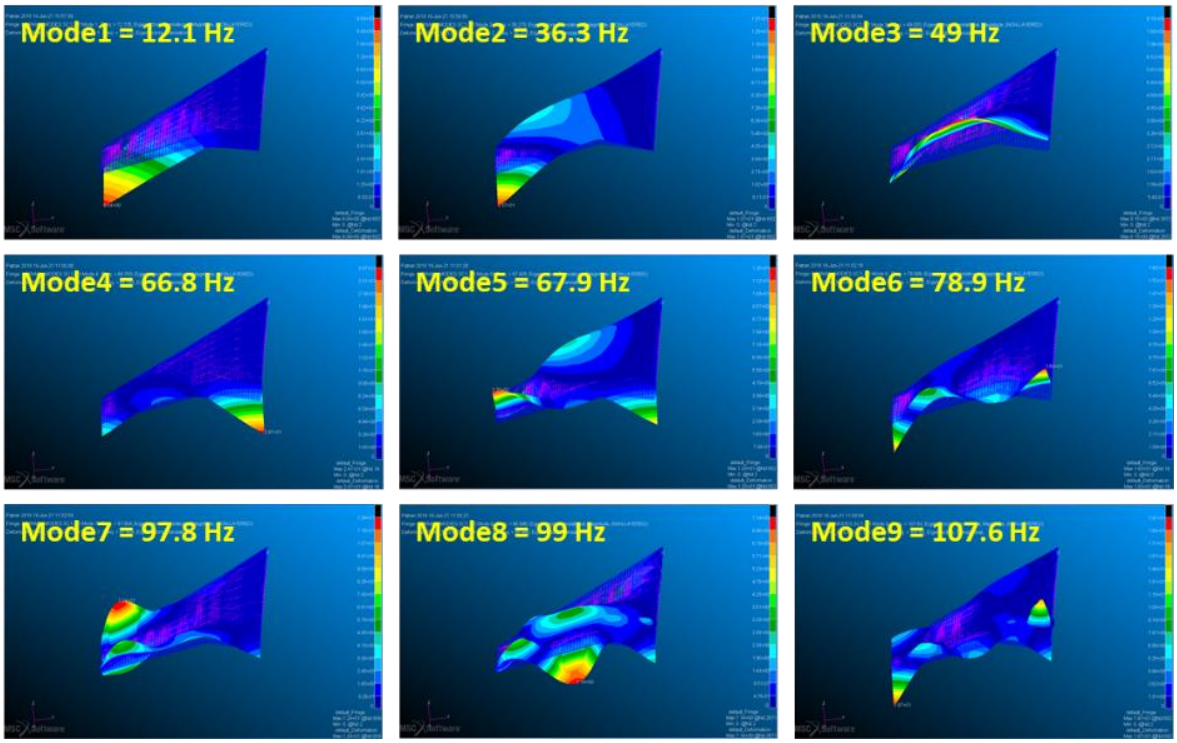

Figure 6: Modal analysis of updated FE model with “0” degree UD angle orientation.

4 OPTIMISATION METHOD

For the aeroelastic tailoring optimisation of large-scale models, the optimisation method, required design objectives, design variables, design responses and design constraints are important parameters to be considered before starting the optimisation process. Genetic and gradient based algorithms are commonly used methods in aeroelastic tailoring optimisation [5,6,12]. In this study, a gradient-based algorithm has been selected and an in-house passive aeroelastic tailoring optimisation code has been developed using MATLAB 2020a coupled with the Nastran 2018 gradient-based optimiser at University of Bristol.

The design objective is defined as minimising the wing weight subject to structural, aeroelastic and manufacturing constraints. Therefore, it is a "single objective multi-disciplinary" optimisation problem. The design variables are the polynomial coefficients of ply angle orientation and quadratic thickness functions, which are independent for the upper and lower skins. The design responses are the static and buckling analyses, which are employed to compute stresses, strains, wing tip twist and 1st buckling mode reserve factor. The design constraints used in the aeroelastic tailoring of the combat aircraft wing are determined as weight, stress, strain, wing tip twist, buckling and minimum skin thickness.

The aerodynamic loads from subcases 1000, 2000, 3000 and 4000 and fuel loads, shown in Table 3, are used in the aeroelastic tailoring optimisation of the updated FE model presented in section 3. The final load formulated in section 3.2, which is 1.5 x (Aerodynamic + Fuel Loads), are included in the optimisation study. Optimisation study constraints for the passive aeroelastic wing tailoring are given in Table 7. It should be noted the tip twist difference constraint presented in this table is the absolute tip twist difference between the Subcases 1000 and 2000.

Table 7: Optimisation study constraints.

Constraints	Value
Maximum tensile strain on composite skin [με]	5500
Maximum compression strain on skin [με]	-3000
Maximum tensile stress on Aluminium substructure [MPa]	446
Maximum compression stress on Aluminium substructure [MPa]	-391
Maximum shear stress on Aluminium substructure [MPa]	280
Buckling reserve factor	1
Maximum tip twist difference [deg]	5.5
Minimum composite skin thickness [mm]	2.4

Passive aeroelastic tailoring wing optimisation is considered with black metal (BM), unidirectional (UD), 1D Variable Angle Tow (VAT) and 2D Variable Angle Tow (VAT) configurations. Among these configurations, black metal is the baseline case. Angle orientation of UD and 1D VAT configurations are as a function of spanwise position, whereas it is implemented as a function of spanwise and chordwise position for the 2D VAT.

4.1 Computation of Centroids

The centroid of each element in the structural FE model is computed to produce the shape of composite distribution across the wing. The so-called centroid is expressed as

$$x_g = \frac{1}{n}\sum_{i=1}^{n} G_{xi} \qquad y_g = \frac{1}{n}\sum_{i=1}^{n} G_{yi} \tag{2}$$

where "x_g" and "y_g" represent the centroid of a 2D CQUAD4 and CTRIA3 elements in the chordwise (x) and spanwise (y) directions, respectively. Similarly, G_x and G_y represent the coordinates of the grid points in chordwise (x) and spanwise (y) directions, respectively.

4.2 Composite Skin Thickness Distribution

In this study, the skin thickness is defined as a function of the normalised span ($0 \rightarrow 1$), using quadratic polynomial function to vary the thickness from wing root to tip. The representative span of a normalised mapping of the wing is shown in Figure 7, where points 1, 2, 3, 4 and 5 are the control points along the span.

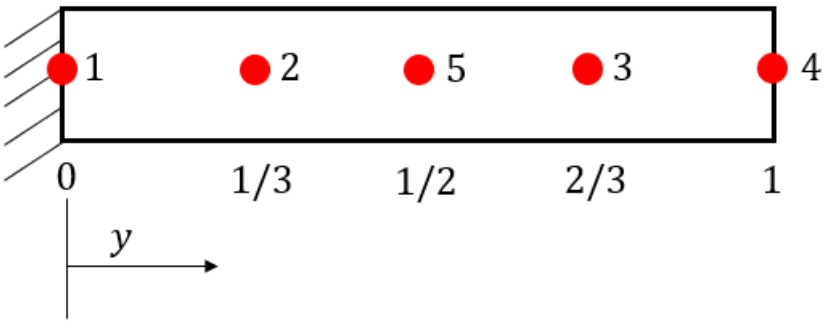

Figure 7: Control points along span of the representative wing.

The quadratic polynomial function for the composite skin thickness is expressed as

$$T(y) = K + My + Py^2 \tag{3}$$

where K, M and P represent unknown polynomial coefficients which are part of the variables used in the optimisation process. Initial values of polynomial coefficients of quadratic skin thickness equation are determined based upon preliminary thickness values at the control points, with T_1, T_4, T_5 representing the initial skin thickness defined at the wing root, wing tip and middle of the span, are inserted into Eq. 3. The resulting matrix equations can be written as

$$\begin{bmatrix} 0 & 0 & 1 \\ 1/4 & 1/2 & 1 \\ 1 & 1 & 1 \end{bmatrix} \begin{bmatrix} P \\ M \\ K \end{bmatrix} = \begin{bmatrix} T_1 \\ T_5 \\ T_4 \end{bmatrix}. \tag{4}$$

from which it is possible to compute the required initial values of P, M and K.

4.3 Black Metal (BM) Optimisation

In the black metal configuration, the composite skin laminate is composed of a stack with 25% 0° / 25% 90°/ 50% ± 45° fibres, leading to quasi-isotropic behaviour. As a result, there is no fibre-steering of the composite laminates, and the constant angle orientation is written as

$$\theta(y) = 0 \tag{5}$$

The original wing model presented in section 2 has the same ply proportion as the black metal configuration. The original ply angle stacking sequence is therefore defined as

(0, 45, 90, -45, 0, 45, 90, -45, 0, 45, 90, -45 / SYM).

and this black metal case is used as the baseline reference for the optimisation studies.

4.4 Unidirectional (UD) Optimisation

UD optimisation is achieved by defining a constant ply angle orientation along the wing span. This approach leads to bend-twist coupling on the wing, and as a result changing structural and aeroelastic behaviour. The unidirectional ply angle orientation is written as

$$\theta(y) = A. \tag{6}$$

where A is the design variables for the ply angle orientation. For the unidirectional optimisation study, the ply angle stacking sequence is defined as

(0, 90, 0, 45, 0, -45, 0, 90, 0, 45, 0, -45/ SYM).

With this ply angle stacking sequence, the ply proportion becomes 50% "0", which is similar to the stacking sequence given in section 3. It should be noted that this ply angle stacking sequence is also used for the 1D and 2D variable angle tow optimisation in sections 4.5 and 4.6

4.5 1D Variable Angle Tow (VAT) Optimisation

Variable angle tow steering optimisation is achieved by rotating the orthotropic laminate along the span. Rather than defining the orientations for each individual element and thus having an enormous number of optimisation variables, and also to facilitate a smooth shape that is manufacturable, the fibre steered (variable angle tow) aeroelastic optimisation employed cubic polynomial shape functions to define the ply angle orientations along the wing span (1D optimisation as a normalised function of span (x) $0 < x < 1$), which can be written as

$$\theta(y) = A + Cy + Fy^2 + Jy^3 \tag{7}$$

where, A, C, F and J are polynomial coefficients represent the design variables for the ply angle orientation, similar to the composite skin thickness function in Eq. 3. Note that the relative orientations between the plies remains the same, but they are all rotated by the angle "θ". The first derivative of the polynomial function can also be employed to control the angle variation along the wing which is important for the manufacturing constraints in practice (limit on the rotation angle of the tows). The first derivative of the polynomial function is written as

$$\frac{\partial \theta}{\partial x} = C + 2Fy + 3Jy^2. \tag{8}$$

The gradient based approach used in this study requires initial conditions to be defined and, in a similar way to the method used to prime the thickness variations, the initial values of the ply

angle orientation at the root θ_0 (0), one third θ_1 (1/3) and two thirds θ_2 (2/3) and the tip θ_3 (1), span length of the wing have to be defined, as shown in Figure 7.

By defining initial orientation values θ_i, the initial values of the polynomial coefficients can be determined using the expression

$$\begin{bmatrix} 0 & 0 & 0 & 1 \\ \frac{1}{27} & \frac{1}{9} & \frac{1}{3} & 1 \\ \frac{8}{27} & \frac{4}{9} & \frac{2}{3} & 1 \\ 1 & 1 & 1 & 1 \end{bmatrix} \begin{bmatrix} J \\ F \\ C \\ A \end{bmatrix} = \begin{bmatrix} \theta_1 \\ \theta_2 \\ \theta_3 \\ \theta_4 \end{bmatrix} \tag{9}$$

4.6 2D Variable Angle Tow (VAT) Optimisation

Variable angle tow steering can also be achieved by varying the ply angles consecutively along both chordwise (x) and spanwise (y) directions. For this purpose, a more complex definition of the ply angle orientation is required as a function of span (y) and chord (x). The mathematical model for the ply angle orientation along the wing chord and span can be written as

$$\theta(x, y) = A + Bx + Cy + Dx^2 + Exy + Fy^2 + Gx^2y + Hy^2x + Ix^3 + Jy^3. \tag{10}$$

Eq. 10 is in the form of three-degree polynomial with two variables, enabling the basis of the 2D VAT optimisation. A representative mapping of the wing model for the 2D VAT optimisation is shown in Figure 8, where the positions 1 to 10 are the control points defined along the chord and span. Using a similar approach to that of the thickness and 1D VAT optimisation methodologies, a 10x10 set of simultaneous equations is arrived using Eq. 10 for each of the control points from which the initial values of the polynomial coefficients in Eq. 10 can be computed.

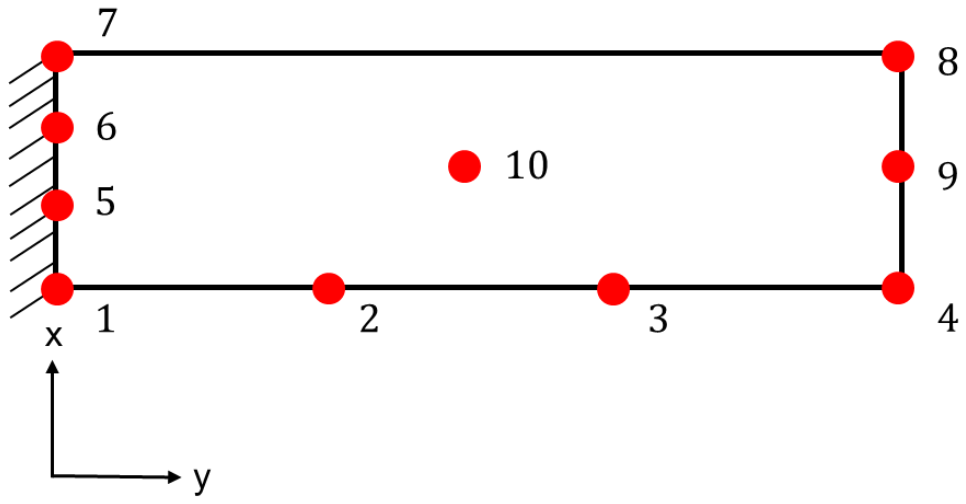

Figure 8: Control points distribution on the representative wing for 2D VAT.

5 OPTIMISATION CASE STUDIES

In this section, the final results of the optimisation case studies for black metal, unidirectional, 1D and 2D variable angle tow steering are presented. The design objective is set as minimising the total weight of wing subject to structural, aeroelastic and manufacturing constraints, as explained in optimisation methodology in section 4. The design variables are the polynomial coefficients of ply angle orientation and thickness functions which are independent for the upper and lower skins. The design responses are the static and buckling analyses employed to compute stresses, strains, tip twist and 1st buckling mode reserve factor. The design constraints, given in Table 7 are employed, for the design responses stated above. Ply angle stacking sequences for black metal, unidirectional and 1D/2D variable angle tow configurations and aerodynamics loads presented in the wing modal description section, provided in Table 3, are also considered.

Table 8: Optimisation case studies.

Configuration	Case Study #	Angle Orientation Function	Skin Thickness Function
Black Metal - Reference	1A	N/A	Quadratic
Unidirectional	3A	Constant (Degree 0 in variable 1)	Quadratic
1D Variable Angle Tow	5A	Cubic (Degree 3 in variable 1)	Quadratic
2D Variable Angle Tow	8A	Cubic (Degree 3 in variable 2)	Quadratic

The case studies presented in this section are listed in Table 8, including their configuration, angle orientation and skin thickness functions.

5.1 Black Metal (CS-1A)

In Case Study - 1A, the composite laminates are set as quasi-isotropic, often referred to as black metal. The black metal configuration (equal 0^o / 90^o / $\pm 45^o$) is taken as the baseline reference model for this study and is used in the comparisons between unidirectional and 1D/2D variable angle tow optimisations. Due to the symmetries in the black metal configuration, which can be assumed to be isotropic, only the polynomial coefficients of the quadratic skin thickness are optimised.

Based on the initial skin thickness values, the in-house passive aeroelastic tailoring optimisation code is used to determine the polynomial coefficients of the quadratic skin thickness distribution and then the optimisation is started. The final weight of the black metal optimisation is computed as 1772.8 kg.

5.2 Unidirectional (CS-3A)

Case Study - 3A aims to investigate the use of unidirectional ply angle orientation optimisation with a quadratic composite skin thickness. The final weight is computed as 1443.9 kg, providing a 18.6 % weight reduction with respect to the black metal configuration. Optimised results for the composite ply angle orientation are presented in Figure 9. The optimised values of the ply angle orientation for the upper and lower skins are computed as -18.7^o and $+10.9^o$, respectively.

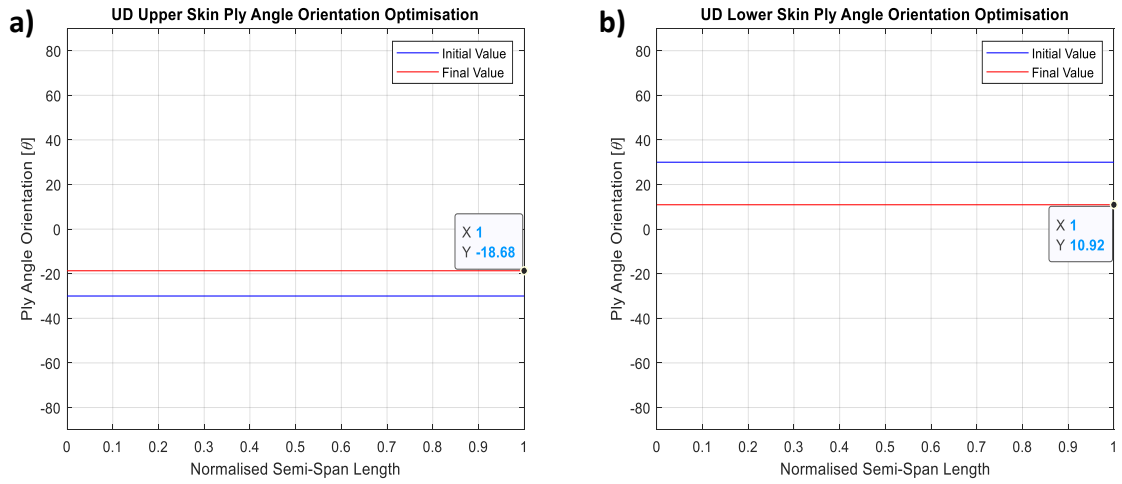

Figure 9: UD ply angle variation, a) upper skin, b) lower skin.

5.3 1D Variable Angle Tow (CS-5A)

In this case study, 1D variable angle tow (VAT) ply angle orientation with quadratic composite skin thickness is employed for the optimisation of the combat aircraft wing. The optimised final weight is computed as 1260.1 kg, leading to a weight reduction of 28.9% compared to the black metal baseline. By using the optimised polynomial coefficients, the ply angle variations of upper and lower skins along the wing span are plotted in Figure 10.

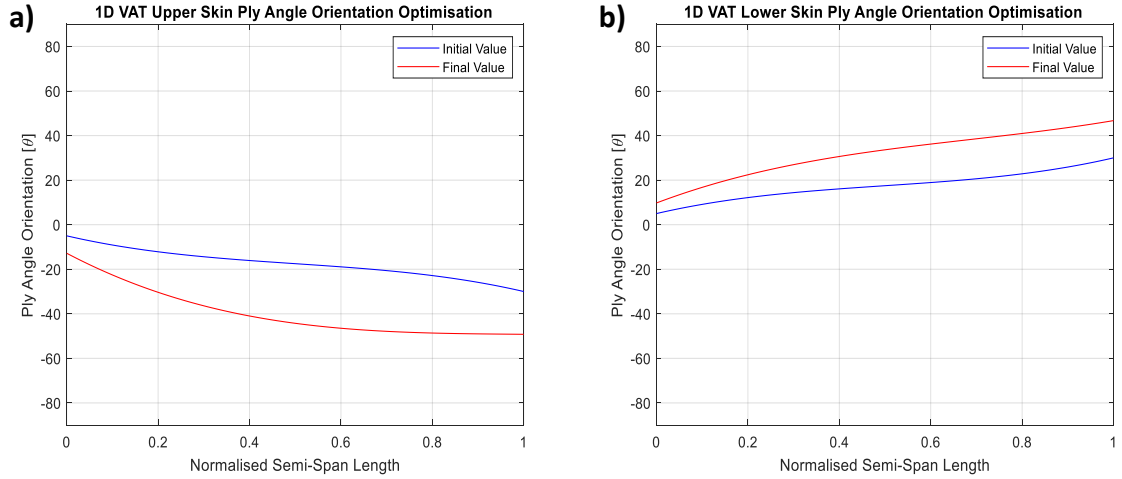

Figure 10: 1D VAT ply angle variation, a) upper skin, b) lower skin.

5.4 2D Variable Angle Tow (CS-8A)

In this case study, a 2D variable angle tow (VAT) ply angle orientation with quadratic composite skin thickness is employed. The optimised final weight is computed as 1155.7 kg, leading to significant weight reduction of 34.8% compared to the black metal configuration. For the upper and lower composite skin, the optimized composite ply angle orientation along the wing chord and span are shown in Figure 11.

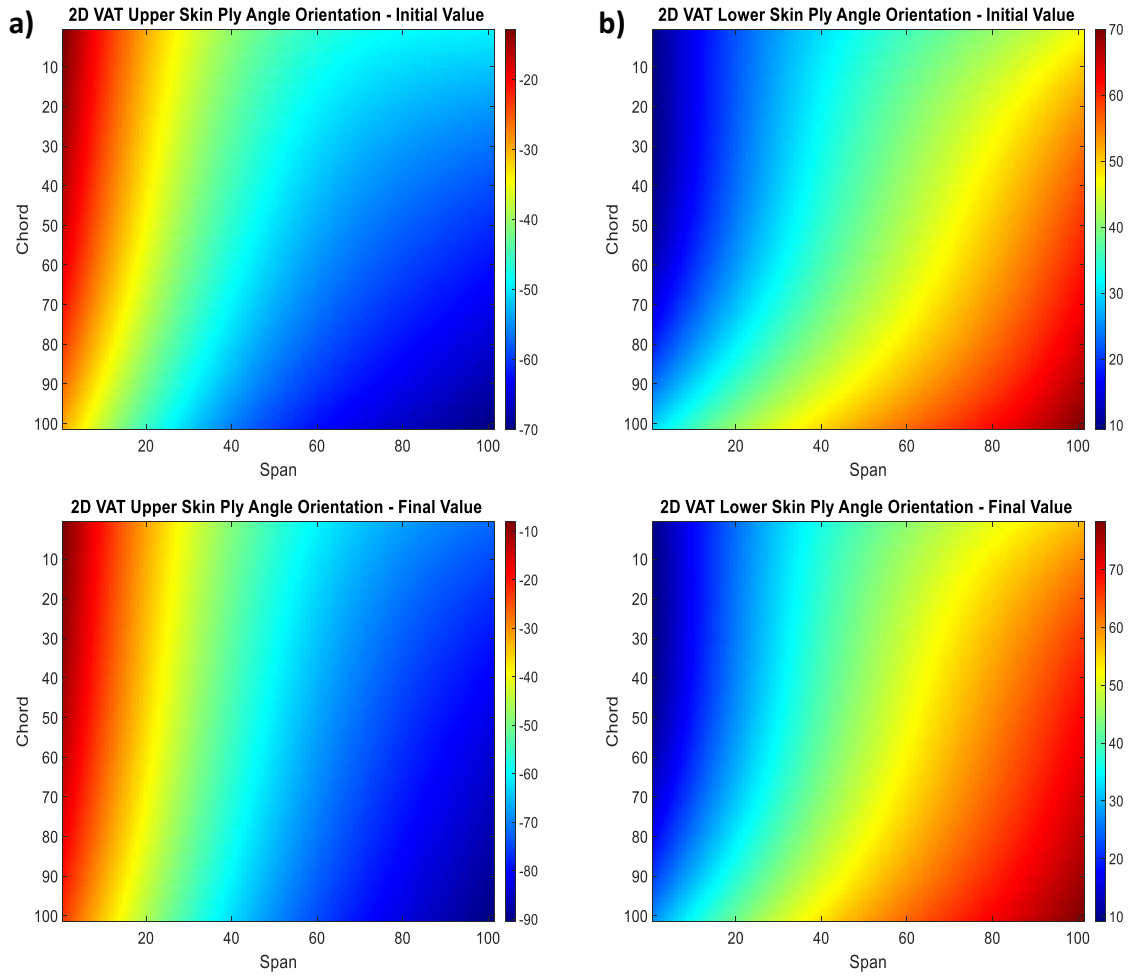

Figure 11: 2D VAT ply angle variation, a) upper skin, b) lower skin.

5.5 Comparison of Results

The final results of the optimisation case studies for black metal, unidirectional, 1D and 2D variable angle tow steering are presented. All the optimisation case study results in terms of total weight, weight reduction, tip twist difference between subcase 1000 and 2000 and 1st buckling reserve factor (RF) are summarised in Table 9, allowing easy comparison between the cases.

Table 9: Optimised results.

Configuration	Case Study #	Total Weight [kg]	Weight Reduction %	Tip Twist Difference [deg]	1st Buckling RF
Black Metal - Reference	1A	1772.8	N/A	2.08	5.62
Unidirectional	3A	1443.9	18.6	2.87	5.69
1D Variable Angle Tow	5A	1260.1	28.9	1.84	4.34
2D Variable Angle Tow	8A	1155.7	34.8	1.93	2.93

It is found that UD, 1D VAT and 2D VAT achieved 18.6%, 28.9% and 34.8% weight reduction with respect to the black metal reference configuration. Based on the final results of the optimisation case studies, the composite strain is found to be the main critical constraint in all configurations, reaching its maximum value given in Table 7. Similarly, the shear stress on the

Aluminium substructure becomes another critical constraint for the 1D and 2D VAT configurations.

6 CONCLUSIONS

An investigation to consider the possibility of employing tailored unidirectional and fibre steered aeroelastically tailored composite lay-up techniques for a combat aircraft wing to meet performance requirements (maximise lift/drag) at more than one design condition has been performed. Modal analysis and aeroelastic analyses were carried out to investigate the structural and aeroelastic behaviour of the combat aircraft wing structure and to determine the initial design space. A passive aeroelastic tailoring optimisation methodology, including black metal, unidirectional, 1D variable angle tow and 2D variable angle tow steering, was created and implemented using MATLAB 2020a and Nastran 2018 to create an in-house passive aeroelastic tailoring optimisation code.

Four different flight conditions were considered with their corresponding aerodynamic loads applied to the structure directly. Black metal (BM), Unidirectional (UD), 1D Variable Angle Tow (VAT) and 2D Variable Angle Tow (VAT) optimisation studies were successfully completed under stress, strain, twist, buckling and manufacturing constraints. The main findings are:

- The weight of the combat aircraft wing can be reduced with both aeroelastically tailored UD, 1D VAT and 2D VAT composite skins.
- For the minimum composite skin thickness 2.4 mm, weight reduction for the UD, 1D VAT and 2D VAT cases can be achieved as 18.6%, 28.9% and 34.8%, respectively when using the black metal optimisation case as a reference. Likewise, tip twist difference for the UD, 1D VAT and 2D VAT cases can be achieved as 2.9^{o}, 1.8^{o} and 1.9^{o}, respectively.
- Composite strain and aluminium shear stress are found to be the critical constraints in 1D and 2D VAT aeroelastic optimisation, which mainly dominate the results.

This study has demonstrated the potential usage of 1D or 2D variable angle tow steering in future combat aircraft wing designs.

7 REFERENCES

[1] M.H. Shirk, T.J. Hertz, T.A. Weisshaar, Aeroelastic Tailoring - Theory, Practice, and Promise., J. Aircr. 23 (1986) 6–18. https://doi.org/10.2514/3.45260.

[2] P. Veers, G. Bir, D. Lobitz, Aeroelastic Tailoring in Wind-Turbine Blade Applications, in: Wind. 1998, Am. Wind Energy Assoc. Meet. Exhib., 1998. http://www.osti.gov/energycitations/product.biblio.jsp?osti_id=672151.

[3] N.J. Krone, Divergence elimination with advanced composites, in: Aircr. Syst. Technol. Meet., American Institute of Aeronautics and Astronautics, Reston, Virigina, 1975. https://doi.org/10.2514/6.1975-1009.

[4] T.A. Weisshaar, Aeroelastic Tailoring of Forward Swept Composite Wings, J. Aircr. 18 (1981) 669–676. https://doi.org/10.2514/3.57542.

[5] O. Stodieck, J.E. Cooper, P.M. Weaver, P. Kealy, Optimization of tow-steered composite wing laminates for aeroelastic tailoring, AIAA J. 53 (2015) 2203–2215. https://doi.org/10.2514/1.J053599.

[6] O. Stodieck, J.E. Cooper, P.M. Weaver, P. Kealy, Aeroelastic tailoring of a

representative wing box using tow-steered composites, AIAA J. 55 (2017) 1425–1439. https://doi.org/10.2514/1.J055364.

[7] O. Stodieck, G. Francois, D. Heathcote, E. Zympeloudis, B.C. Kim, A.T. Rhead, D. Cleaver, J.E. Cooper, Experimental validation of tow-steered composite wings for aeroelastic design, 17th Int. Forum Aeroelasticity Struct. Dyn. IFASD 2017. 2017–June (2017) 1–16.

[8] M. Capuzzi, A. Pirrera, P.M. Weaver, Structural design of a novel aeroelastically tailored wind turbine blade, Thin-Walled Struct. 95 (2015) 7–15. https://doi.org/10.1016/j.tws.2015.06.006.

[9] S. Scott, M. Capuzzi, D. Langston, E. Bossanyi, G. McCann, P.M. Weaver, A. Pirrera, Effects of aeroelastic tailoring on performance characteristics of wind turbine systems, Renew. Energy. 114 (2017) 887–903. https://doi.org/10.1016/j.renene.2017.06.048.

[10] S.M. Barr, J.W. Jaworski, Optimization of tow-steered composite wind turbine blades for static aeroelastic performance, Renew. Energy. 139 (2019) 859–872. https://doi.org/10.1016/j.renene.2019.02.125.

[11] B.C. Kim, K. Potter, P.M. Weaver, Continuous tow shearing for manufacturing variable angle tow composites, Compos. Part A Appl. Sci. Manuf. 43 (2012) 1347–1356. https://doi.org/10.1016/j.compositesa.2012.02.024.

[12] O. Stodieck, Aeroelastic Tailoring of Tow-Steered Composite Wings, Ph.D. Thesis, University of Bristol, Bristol, UK, 2016. https://doi.org/10.13140/RG.2.2.29020.82562.

[13] B. Smith, T. Brooks, M. Leader, T.W. Chin, G. Kennedy, J. Martins, C. Cesnik, Passive Aeroelastic Tailoring, Contractor Report, NASA, USA, 2020.

[14] F.E. Eastep, V.A. Tischler, V.B. Venkayya, N.S. Khot, Aeroelastic tailoring of composite structures, J. Aircr. 36 (1999) 1041–1047. https://doi.org/10.2514/2.2546.

[15] H.F. Seibert, Applications for PMI foams in aerospace sandwich structures, Reinf. Plast. 50 (2006) 44–48. https://doi.org/10.1016/S0034-3617(06)70873-6.

[16] L. Zhu, N. Li, P.R.N. Childs, Light-weighting in aerospace component and system design, Propuls. Power Res. 7 (2018) 103–119. https://doi.org/10.1016/j.jppr.2018.04.001.

[17] A. Kausar, Polyurethane Composite Foams in High-Performance Applications: A Review, Polym. - Plast. Technol. Eng. 57 (2018) 346–369. https://doi.org/10.1080/03602559.2017.1329433.

[18] P. Jadhav, Innovative designs of embedded foam inserts in aerospace composite structures, Mater. Today Proc. 21 (2020) 1164–1168. https://doi.org/10.1016/j.matpr.2020.01.066.

ACKNOWLEDGEMENT

The authors from the University of Bristol are therefore grateful to BAE Systems for providing the financial support for this project.

COPYRIGHT STATEMENT